BRL-CR-0600

FILE COPY

CONTRACT REPORT BRL-CR-0600

BRL

1938 – Serving the Army for Fifty Years – 1988

AN ATTEMPT TO RECONCILE COMPRESSION SENSITIVITY DATA ON LIQUID GUN PROPELLANTS

NEALE A. MESSINA

JUNE 1988

U.S. ARMY LABORATORY COMMAND

BALLISTIC RESEARCH LABORATORY

ABERDEEN PROVING GROUND, MARYLAND

DESTRUCTION NOTICE

Destroy this report when it is no longer needed. DO NOT return it to the originator.

UNCLASSIFIED
SECURITY CLASSIFICATION OF THIS PAGE

REPORT DOCUMENTATION PAGE

Form Approved
OMB No. 0704-0188

1a. REPORT SECURITY CLASSIFICATION Unclassified	1b. RESTRICTIVE MARKINGS
2a. SECURITY CLASSIFICATION AUTHORITY	3. DISTRIBUTION / AVAILABILITY OF REPORT Approved for public release; distribution unlimited.
2b. DECLASSIFICATION / DOWNGRADING SCHEDULE	
4. PERFORMING ORGANIZATION REPORT NUMBER(S) PCRL-FR-88-003	5. MONITORING ORGANIZATION REPORT NUMBER(S)
6a. NAME OF PERFORMING ORGANIZATION Princeton Combustion Research Laboratories, Inc. 6b. OFFICE SYMBOL (If applicable)	7a. NAME OF MONITORING ORGANIZATION U.S. Army Ballistic Research Laboratory
6c. ADDRESS (City, State, and ZIP Code) 4275 U.S. Highway One Monmouth Junction, NJ 08852	7b. ADDRESS (City, State, and ZIP Code) Aberdeen Proving Ground, MD 21005-5066
8a. NAME OF FUNDING / SPONSORING ORGANIZATION U.S. Army Ballistic Rsch Lab 8b. OFFICE SYMBOL (If applicable) SLCBR-IB	9. PROCUREMENT INSTRUMENT IDENTIFICATION NUMBER DAAD05-86-M-M414
8c. ADDRESS (City, State, and ZIP Code) Aberdeen Proving Ground, MD 21005-5066	10. SOURCE OF FUNDING NUMBERS PROGRAM ELEMENT NO. / PROJECT NO. / TASK NO. / WORK UNIT ACCESSION NO.

11. TITLE (Include Security Classification)

AN ATTEMPT TO RECONCILE COMPRESSION SENSITIVITY DATA ON LIQUID GUN PROPELLANTS

12. PERSONAL AUTHOR(S)
Neale A. Messina

13a. TYPE OF REPORT	13b. TIME COVERED	14. DATE OF REPORT (Year, Month, Day)	15. PAGE COUNT
Final	FROM 2/86 TO 3/86		

16. SUPPLEMENTARY NOTATION

17. COSATI CODES		
FIELD	GROUP	SUB-GROUP

18. SUBJECT TERMS (Continue on reverse if necessary and identify by block number)
Compression Ignition Liquid Gun Propellants Hazards
Liquid Propellant Guns Adiabatic Compression

19. ABSTRACT (Continue on reverse if necessary and identify by block number)

This report is an attempt to reconcile apparent discrepancies between conclusions drawn from compression ignition sensitivity test results of liquid gun propellants obtained independently by Princeton Combustion Research Laboratories, Inc. (PCRL) and Ernst-Mach-Institut, Abteilung fur Ballistik (EMI-AFB). Here we define compression ignition as an undesirable ignition event arising from hot spot development associated with entrapped bubble collapse under rapid compression of the liquid propellant charge.

20. DISTRIBUTION / AVAILABILITY OF ABSTRACT ☐ UNCLASSIFIED/UNLIMITED ☒ SAME AS RPT. ☐ DTIC USERS	21. ABSTRACT SECURITY CLASSIFICATION Unclassified	
22a. NAME OF RESPONSIBLE INDIVIDUAL John D. Knapton	22b. TELEPHONE (Include Area Code) (301) 278-6170	22c. OFFICE SYMBOL SLCBR-IB-B

DD Form 1473, JUN 86   Previous editions are obsolete.   SECURITY CLASSIFICATION OF THIS PAGE

UNCLASSIFIED

PRINCETON
COMBUSTION
RESEARCH
LABORATORIES, INC.

AN ATTEMPT TO RECONCILE COMPRESSION SENSITIVITY DATA
ON LIQUID GUN PROPELLANTS

PRINCETON COMBUSTION RESEARCH LABORATORIES, INC.
4275 U.S. HIGHWAY ONE, MONMOUTH JUNCTION, NEW JERSEY 08852 TELEPHONE: (609) 452-9200

Final Report PCRL-FR-88-003
April 15, 1988

AN ATTEMPT TO RECONCILE COMPRESSION SENSITIVITY DATA ON LIQUID GUN PROPELLANTS

Princeton Combustion Research Laboratories, Inc.
4275 U.S. Highway One
Monmouth Junction, NJ 08852

in fulfillment of
the Reporting Requirements on

DAAD05-86-M-M414

U.S. Army Ballistic Research Laboratory
Aberdeen Proving Ground, MD 21005-5066

TABLE OF CONTENTS

LIST OF TABLES

LIST OF FIGURES

INTRODUCTION

Safe start-up and operation of a liquid propellant gun (LPG) system can be accomplished if the relevant sensitivity parameters of the candidate monopropellant as relates to compression ignition can be identified. It is essential that a quantitative characterization of the threshold for runaway reaction associated with compression ignition be established and brought under precise control in LPG design. As a practical approach to defining the domain of safe start-up for LPG operation, it is necessary to provoke runaway reactions, i.e., explosions, in a specialized reusable laboratory-scale test fixture. It must also be recognized that residual ullage and cavitation bubbles brought into the liquid reservoir of a LPG during the pre-firing rapid fill process will influence the sensitization of the liquid monopropellant to compression ignition. It is therefore essential that cavitating flow dynamics induced by the rapid fill process be incorporated into laboratory fixture design, aside from a quiescent or static liquid propellant loading with single or multiple gas pockets or bubbles.

To this end, Princeton Combustion Research Laboratories, Inc. designed and fabricated a Compression Ignition Sensitivity Test Fixture in 1979 to produce on a systematic basis rapid compression of a liquid monopropellant charge, with or without ullage, under rapid fill or quiescent loading conditions (Ref. 1). The sensitivity to compression ignition of various liquid monopropellants has been investigated over the years, including Otto Fuel II, NOS-365, LGP 1845, and LGP 1846 (Ref. 2-4).

As a result of the recognized utility of the PCRL Compression Ignition Sensitivity Test Fixture in establishing the hazards potential of liquid gun propellants to rapid compression stimulus, Dr. E. Schmolinske of Fraunhofer Institut fur Kurzzeitdynamik, Ernst-Mach-Institut, Abteilung fur Ballistik (EMI-AFB) undertook an effort to design and test a windowed, high pressure, rapid compression apparatus modeled after the PCRL design (Ref. 5). The ability of the EMI-AFB compression apparatus to provide viewing access to the sample volume undergoing rapid compression for high speed cinematography of the dynamics of the bubble compression process is a design feature not present in the PCRL apparatus. Of course, there are other inherent differences in apparatus design which are addressed in this report.

The purpose of this report is an attempt to reconcile apparent discrepancies between conclusions drawn from compression ignition sensitivity data of liquid gun propellants obtained independently by PCRL and by EMI-AFB.

DISCUSSION

Figure 1 shows a functional schematic drawing of the PCRL Compression Ignition Sensitivity Test Fixture. The rapid fill sequence is initiated by activating a circuit that opens the Solenoid Valve which releases the driving N_2 pressure into the 0.5 inch diameter bore of the Pneumatic Load Cylinder to accelerate the Pneumatic Piston. The motion of the Pneumatic Piston forces the liquid propellant and any gas ullage past the Poppet Valve. The liquid propellant and gas ullage flow through the Flow Guide, possibly resulting in cavitation depending on the nature of the orifice, into the bore of the Compression Chamber. The Projectile Piston is then driven to the right allowing the LP charge (6.65 cm^3) to fill the bore until maximum stroke is achieved. The contact of the Projectile Piston with the contact wire in the End Plug completes a circuit that fires an M52 Electric Primer in the Starter Charge Chamber. The resulting pressure generated by the combustion of the tailored smokeless powder starter charge is sensed by the Compression Piston which is free to move in the Compression Chamber bore. As the pressure in the Starter Charge Chamber rises, the Compression Piston accelerates compressing the liquid propellant charge and the embedded bubbles. If the liquid propellant charge undergoes runaway reaction at some point in the compression cycle, the Projectile Piston will shear through the aluminum shear disc when the bore pressure exceeds 450-480 MPa (65-70 kpsi). PCB type 119A quartz pressure transducers, ruggedized to withstand hydraulic pressures to 200 kpsi, are mounted in the Compression Chamber to record pressure-time histories in the liquid during a compression test. PCRL light sensor assemblies are incorporated in the Compression Chamber for detecting ignition of the liquid propellant charge.

The EMI-AFB test fixture is shown schematically in Figure 2. The liquid propellant sample (14 cm^3) is introduced into the sample cavity as a quiescent liquid, i.e., static fill. A bubble generating device located below the liquid propellant sample cavity introduces discrete bubbles into the sample. The compression sequence is then initiated by an electric primer firing into the upper combustion chamber. The pressure generated acts on the face of the driving (compression) piston and, once the restraining shear pin fails, piston motion ensues, compressing the liquid propellant charge and the embedded bubbles. The compression piston is of a differential area hydraulic intensifier design. The test fixture is configured with optical windows to observe the bubble collapse phenomenon through high speed cinematography, and with a pressure transducer for monitoring the pressure-time history in the liquid propellant during a compression test.

Table 1 presents a comparison of the PCRL device and the EMI-AFB device before and after recent modifications to the latter fixture. The most striking difference between the two fixtures is the state of the liquid propellant and associated ullage at the onset of rapid compression. In the PCRL

Compression Ignition Sensitivity Test Fixture, the initial condition is a pre-pressurized liquid propellant charge containing a homogeneously distributed field of microbubbles with mean bubble diameter less than 0.0025 cm. This is meant to simulate the pre-firing propellant rapid loading process in the gun, prior to the onset of regenerative piston motion. On the other hand, in the EMI device, the initial condition is a liquid propellant charge at atmospheric pressure in which discrete bubbles of initial mean bubble diameter on the order of 0.1 cm are introduced into the LP field.

The conclusions drawn by Dr. Schmolinske based on his experimental data were that no ignitions attributable to compression ignition were observed at conditions supposedly duplicating those in PCRL experiments (Ref. 5). The one liquid propellant initiation observed was thought to be a result of friction and viscous heating in the small annular clearance where the bubble generating device is located. The question arises: why the apparent discrepancy in results? It is PCRL's belief that no contradictions exist and, in fact, the EMI data support the PCRL data.

To summarize the reconciliation of the two data sets, before getting into the details of analysis of each test, let us offer the following explanation. Of paramount importance is the fact that the liquid pressurization rate upon which the PCRL compression ignition sensitivity data correlates is the <u>mean</u> pressurization rate, not the instantaneous <u>maximum</u> pressurization rate. Upon inspecting expanded scale pressure-time plots from EMI tests, it is observed that the mean pressurization rate is less than that corresponding to TYPE "C" start-up in PCRL experiments, i.e., nominally 200 MPa/msec, in which the liquid response was benign for NOS-365 and for LGP-1845. So it would be anticipated, based on considerations of mean liquid pressurization rate only, that the response of the bubbly propellant charge in EMI tests would also be benign. However, there is another consideration. The bubble diameter in EMI tests is approximately a factor of 40 larger than in PCRL tests and it has always been PCRL's contention that the presence of larger bubbles sensitizes the liquid propellant to hot spot development to a greater extent than smaller diameter bubbles. This is still held to be true provided that the bubbles undergo collapse without significant deformation during pressurization leading to splitting and shattering. In the EMI experiments the large diameter bubbles introduced into the LP field appear hydrodynamically unstable under the action of the pressure wave motion, undergoing splitting and shattering for high initial liquid pressurization rates. It is doubtful whether the bubble internal (gas and vapor) pressure is maintained in each bubble fragment as splitting and shattering occurs from the parent bubble. It is hypothesized that the bubble shattering mechanism relieves the internal bubble pressure so that the instantaneous overpressure across the bubble boundary, delta-p, is relieved. Thermodynamic effects, i.e., average internal temperature, associated with hot spot development due to bubble compression

would be reduced. That is to say, it is speculated that the maximum internal temperature attained is less for a bubble that has undergone asymmetric collapse, splitting, and shattering, than for one that collapses without shattering.

Thus, the lower mean liquid pressurization rate in EMI tests, the bubble shattering mechanism observed in EMI tests with high initial liquid pressurization rates, and/or a combination of both is responsible for the observed benign response of the bubbly liquid monopropellant subjected to rapid compression in EMI tests. PCRL test results and EMI test results are consistent when compared on this basis.

High speed films of EMI tests designated 18-4-85, LPG 1845; 6-4-85, NOS-365; and 31-4-84, NOS-365 have been analyzed in detail with the aid of a motion analyzer located at U.S. Army BRL. Measurements of bubble sizes have been conducted, frame by frame, to the point where measurement was no longer possible due to resolution limitations. These bubble measurement data were then correlated with liquid pressure p-t data. The high speed cinematography was conducted with a Hitachi camera with a framing rate of 10,000 fps or 0.10 msec per frame. The exposure time per frame was 1.45 microsec. Although additional high speed cinematography was conducted with a Beckman camera, 4.0 microsec per frame and an exposure time of 300 nanosec, these photographic records have not been analyzed.

The EMI high speed bubble collapse photos provide information from one viewing direction only, so that the three dimensional form of the collapse profiles can only be assumed from considerations of symmetry. In those cases where major and minor axes of the bubble are equal, we assume a spherically symmetric bubble. In those cases where major and minor axes differ, two different bodies of revolution can be assumed, an oblate spheroid, i.e., rotation about the minor axis, or a prolate spheroid, i.e., rotation about the major axis. Volumes based on both oblate spheroid gemoetry and prolate spheroid geometry are presented in the accompanying tables for each test. In general, the side view photographs of EMI show a departure from circular profile for rapid liquid pressurization, the bubble collapse manifesting itself in pronounced asymmetry, followed by bubble splitting and bubble shattering.

Test EMI 18-4-85, LP 1845

Only one set of test data is available for LGP 1845 liquid monopropellant. Both high speed cinematographic film and liquid pressure-time data (expanded scale) have been analyzed. Table 2 summarizes bubble size data from the motion analyzer. Initially, single, large diameter bubbles are introduced into the LP. Upon introduction the bubble boundary oscillates somewhat, but the boundary motion damps to produce an ellipsoid-shaped bubble. At the starting condition ($t = 0$), five representative bubbles were identified and tracked in time. The individual bubble volume is in the range of $0.00645 \leq V\ [cm^3] \leq 0.01070$ for oblate spheroid

symmetry and in the range of $0.00547 \leq V\ [cm^3] \leq 0.00869$ for prolate spheroid geometry. At time $t = 0.0001$ sec (second frame), the collapse of the individual bubbles has begun with the bubble boundary retaining its elliptical shape. Volumetric compression of the individual bubbles is approximately 1.2 (see Table 2 for precise numbers). The field pressure, as measured from the expanded pressure-time record of Figure 3, is 20.3 MPa (2.94 kpsi). The field pressure is tabulated as a function of time in Table 3. At time $t = 0.0002$ sec (third frame), continued collapse of the individual bubbles is noted with the bubble boundary still retaining its elliptical shape. Volumetric compression of the individual bubbles is now approximately 3.0. The field pressure is 55.2 MPa (8.01 kpsi). Beyond $t = 0.0002$ sec, between $t = 0.0002$ sec and $t = 0.0003$ sec, continued collapse of the individual bubbles occurs but with boundary distortion. Contrast differences begin to appear in each bubble interior. Bubble labeled No. 5, closest to the wall boundary, is no longer a single, well-defined bubble. At $t = 0.0003$ sec, the field pressure has increased to 97.7 MPa (14.21 kpsi). In the time frame $0.0004 \leq t\ (sec) \leq 0.0005$ bubble splitting can be observed with continued distortion of bubble surfaces. Finally at $t = 0.0006$ sec, with the field pressure equal to 167.6 MPa (24.31 kpsi), shattering of bubbles into localized "mists", i.e., microbubbles, can be observed, persisting for 2.5 to 9.0 msec. During this time interval discrete bubbles are no longer visible. The volumetric compression of individual selected bubbles as a function of time is shown plotted in Figure 4. The sequence of observations from high speed films is indicated on the expanded pressure-time plot of Figure 3.

The compression process did not lead to an ignition event. A detailed look at Figure 3 explains why. During the time interval of maximum pressurization, 420.5 MPa/msec (61.0 kpsi/msec), bubble splitting occurs in the pressure range $97.7 \leq p[MPa] \leq 137.4$, followed by the bubble shattering for $t > 0.5$ msec, for liquid pressure in excess of 162.1 MPa. However, during the time to achieve maximum equilibrium pressure in the liquid ($p = 228$ MPa, 33.1 kpsi), a mean pressurization rate can be identified through the oscillatory character of the start-up p-t curve. This mean pressurization rate is equal to 108.2 MPa/msec (15.7 kpsi/msec). It is this mean pressurization rate that PCRL has identified in its compression sensitivity experiments as one of the important parameters to correlate ignition/no-ignition observations, not the maximum pressurization rate. Table 4 compares tabulated results for EMI test 18-4-85 (no ignition) with "equivalent" PCRL tests A13 and A14 which resulted in no ignition (benign) response of the liquid. Note that the mean liquid pressurization rate in EMI test 18-4-85 is only one-half that in "equivalent" PCRL tests. Comparison is also made with PCRL tests A20, A21, and A24 in which the mean pressurization rate was higher than that in tests A13 and A14 (43 kpsi/msec vs. 31 kpsi/msec). In these PCRL tests with higher higher mean pressurization rate, explosions were observed in two out of three tests.

Also tabulated in Table 4 is the maximum liquid pressurization rate. It is interesting to note that the maximum rate for PCRL tests A13 and A14 is approximately a factor of four greater than for EMI test 18-4-85, yet no explosion was observed. To demonstrate that the maximum liquid pressurization rate is not the correlating factor, PCRL tests A20 and A24 have maximum rates less than A13 and A14 and yet explosions were observed in the former tests! Therefore, on the basis of mean pressurization rate, coupled to the bubble shattering mechanism in EMI tests, the EMI test results and PCRL test results correlate.

Test EMI 6-4-85, NOS-365

One of the available data sets for NOS-365 liquid monopropellant is EMI 6-4-85. Both high speed cinematographic film and liquid pressure-time data have been analyzed. Unfortunately expanded scale p-t data were not made available for this test, so estimates of maximum and mean pressurization rate from the unexpanded record placed these values approximately equal to those experienced in Test 18-5-85. Table 5 summarizes bubble size data from the motion analyzer. The individual bubble volume is in the range of $0.000087 \leq V[cm^3] \leq 0.000487$. This individual bubble volume is a factor of 10 smaller than the bubbles introduced into LGP-1845 in EMI Test 18-5-85. At $t = 0$ single, spherically-symmetric bubbles in close proximity appear in the immediate vicinity of the bubble generator. At $t = 0.0001$ sec, the field pressure has increased to approximately 20.3 MPa (2.94 kpsi). At this time symmetric bubble collapse is evident. At $t = 0.0002$ sec, bubble splitting is observed to occur ($p_L \sim$ 55.2 MPa, 8.01 kpsi). At $t = 0.0003$ sec, bubble shattering is evident. No measureable discrete bubbles exist in the field. This localized collection of microbubble "mist" persists for approximately 1.8 msec. No ignition was observed.

Test EMI 31-4-84, NOS-365

Another available data set for NOS-365 is EMI 31-4-84. This data set differs from Test 6-4-85 in that the mean liquid pressurization rate is reduced by a factor of four, from 420 MPa/msec to 106 MPa/msec. The liquid pressure-time history is shown in Figure 5, with mean pressurization rate approximately equal to maximum pressurization rate. Table 6 tabulates liquid pressure versus time for the first 1.8 msec of bubble collapse. Table 7 summarizes bubble size data from the motion analyzer. In this test the individual bubble volume is in the range of $0.000110 \leq V[cm^3] \leq 0.000885$ for both oblate and prolate spheroid symmetry. As Table 7 indicates, each bubble tracked retains its shape for the duration of the compression process, to the resolution limit of the motion analyzer projector. The volumetric compression of the individual bubbles can be tracked for many frames, owing to the relatively slow pressurization start-up. Volumetric compression factors as high as approximately 30 are noted from the film. The change in individual bubble volume with time is shown in Figure 6. This figure should be compared with volumetric compression results for

bubbly LGP-1845, test EMI 18-5-85, presented in Figure 4. The larger bubble diameter and higher compression rate in Test EMI 18-5-85 result in an accelerating collapse of the bubble until splitting and shattering occurs. Figure 6 demonstrates a completely different collapse behavior for Test 31-4-84, for the case of slow pressurization start-up with bubbles which are one-half to one-third the diameter of those in Test EMI 18-4-85. No bubble shattering is observed to occur. No ignition resulted.

Table 8 compares tabulated results for EMI Tests 6-4-85 and 31-4-84, both of which resulted in no ignition, with "equivalent" PCRL Tests LP06 and LP07 which resulted in no ignition (benign) response of the liquid. Note that the mean liquid pressurization rate in both EMI tests is only one-half that in "equivalent" PCRL tests. Comparison is also made with PCRL Tests LP15, LP16, LP17 and LP18 in which the mean pressurization rate was increased. Three out of four tests resulted in an explosive response.

Again we note that the maximum pressurization rate in PCRL Tests LP06 and LP07 exceeds that in EMI Tests 6-4-85 and 31-4-84 by a factor of approximately 3 for 6-4-85 and a factor in excess of 10 for 31-4-84, yet no explosions were observed in these two PCRL tests. The correlating factor for ignition/no-ignition is the mean pressurization rate.

SUMMARY

- PCRL compression ignition sensitivity data correlate based on mean liquid pressurization rate, not maximum pressurization rate.
- The mean pressurization rates in the three EMI tests discussed in detail in this report are less than that corresponding to TYPE "C" start-up pressurization curve in PCRL tests, nominally 200 MPa/msec (30 kpsi/msec), for which the liquid response was benign.
- The bubble splitting and shattering process observed in several EMI tests tends to further desensitize the liquid.
- Apparent discrepancies between EMI test results and PCRL test results, as voiced by Dr. Schmolinske, have been reconciled.

REFERENCES

1. N.A. Messina, L.S. Ingram, P.E. Camp, and M. Summerfield, "Compression-Ignition Sensitivity Studies of Liquid Monopropellants in a Dynamic-Loading Environment", JANNAF Combustion Meeting, CPIA Publication 308, Vol. I, pp. 247-284, 1979.

2. N.A. Messina, L.S. Ingram and M. Summerfield, "Sensitivity of Liquid Monopropellants to Compression Ignition", JANNAF Combustion Meeting, CPIA Publication 347, Vol. II, pp. 269-287, 1981.

3. N.A. Messina, L.S. Ingram, and M. Summerfield, "Sensitivity of Liquid Monopropellants to Compression Ignition," Princeton Combustion Research Laboratories, Final Report PCRL-FR-83-004, June 1983; also, U.S. Army BRL Contract Report ARBRL-CR-00531, August 1984.

4. N.A. Messina, "Compression Sensitivity of Liquid Monopropellants", U.S.-German Visit on Liquid Propellant Technology at Ballistic Research Laboratory under DEA-1060, 1983.

5. E. Schmolinske, "Bubble Compression in Liquid Propellants", US-German Visit on Liquid Propellant Technology at Ballistic Research Laboratory under DEA-1060, 1983.

	EMI-AFB	
PCRL DEVICE	(ORIGINAL)	(MODIFIED)
RAPID FILL OF LP WITH ASSOCIATED ULLAGE THROUGH POPPET VALVE; FLUID DYNAMIC SUBDIVISION OF ULLAGE	QUIESCENT LP WITH INTRODUCTION OF 0.2 CC ADDITIONAL LP THROUGH INJECTOR ORIFICE PRODUCING CAVITATION BUBBLES	QUIESCENT LP WITH INTRODUCTION OF DISCRETE AIR BUBBLES THROUGH BUBBLE GENERATOR
HOMOGENEOUSLY DISTRIBUTED MICRO-BUBBLES	DISCRETE BUBBLES IN LP FIELD	DISCRETE BUBBLES IN LP FIELD
START-UP TAILORING WITH SOLID PROPELLANT CHARGE	START-UP TAILORING OBTAINED BY ELECTRIC IGNITER AND SHEAR PIN FAILURE	START-UP TAILORING OBTAINED BY ELECTRIC IGNITER AND SHEAR PIN FAILURE
COMPRESSION PISTON FACE IN CONTACT WITH LP	COMPRESSION PISTON FACE IN CONTACT WITH LP	MEMBRANE SEPARATING COMPRESSION PISTON FACE FROM LP CHARGE
PRE-PRESSURIZATION LEVEL OF LP ADJUSTABLE PARAMETER	NO PRE-PRESSURIZATION OF LP	NO PRE-PRESSURIZATION OF LP
DIAGNOSTICS - 3 LIQUID PRESSURE TRANSDUCERS - 3 LIQUID LIGHT SENSORS	DIAGNOSTICS - 1 LIQUID PRESSURE TRANSDUCER - SAPPHIRE VIEWING WINDOW FOR HIGH SPEED CINEMATOGRAPHY	DIAGNOSTICS - 1 LIQUID PRESSURE TRANSDUCER - SAPPHIRE VIEWING WINDOW FOR HIGH SPEED CINEMATOGRAPHY

TABLE 1. Comparison of Features of PCRL Compression Ignition Sensitivity Test Fixture and EMI Device.

$(dp/dt)_{max}$ = 61.0 kpsi/msec
= 420.5 MPa/msec

$(dp/dt)_{mean}$ = 15.7 kpsi/msec
= 108.2 MPa/msec

Bubble No.	B H(cm)	A V(cm)	OBLATE SPHEROID VOL(cm^3)	(V_o/V_b)	PROLATE SPHEROID VOL(cm^3)	(V_o/V_b)	COMMENTS
t = 0							
1	0.238	0.293	0.01070	1	0.00869	1	Single, large bubbles introduced sequentially into LP column; Upon introduction, bubble boundary oscillates somewhat but then becomes ellipsoid and holds shape.
2	0.207	0.244	0.00645	1	0.00547	1	
3	0.213	0.256	0.00731	1	0.00608	1	
4	0.220	0.238	0.00652	1	0.00603	1	
5	0.220	0.256	0.00755	1	0.00649	1	
t = 0.0001 sec	Field Pressure: 200 bar = 2.94 kpsi = 20.3 MPa						
1	0.226	0.268	0.00850	1.259	0.00717	1.212	Collapse of individual bubbles; bubble boundary retains elliptical shape
2	0.195	0.226	0.00521	1.238	0.00450	1.216	
3	0.207	0.244	0.00645	1.133	0.00547	1.112	
4	0.213	0.220	0.00540	1.207	0.00523	1.153	
5	0.213	0.244	0.00664	1.137	0.00580	1.119	
t = 0.0002 sec	Field Pressure: 545 bar = 8.01 kpsi = 55.2 MPa						
1	0.165	0.189	0.00309	3.463	0.00269	3.230	Continued collapse of individual bubbles; bubble boundary retains elliptical shape
2	0.146	0.146	0.00163	3.957	0.00163	3.356	
3	0.159	0.159	0.00210	3.481	0.00210	2.895	
4	0.171	0.146	0.00191	3.414	0.00224	2.692	
5	0.195	0.159	0.00258	2.926	0.00317	2.047	
t = 0.0003 sec	Field Pressure: 967 bar = 14.21 kpsi = 97.7 MPa						Continued collapse of individual bubbles but surface shapes are highly irregular; Contrast differences beginning to appear in each bubble interior; No. 5 bubble no longer single, well-defined bubble.
t = 0.0004 sec	Field Pressure: 1356 bar = 19.93 kpsi = 137.4 MPa						Continued distortion of bubble surfaces; Bubble splitting occurs.
t = 0.0005 sec	Field Pressure: 1600 bar = 23.52 kpsi = 162.1 MPa						Continued distortion of bubble surfaces; Continued bubble splitting.
t = 0.0006 sec	Field Pressure: 1654 bar = 24.31 kpsi = 167.6 MPa; (dp/dt) < 0, 0.05 msec after first pressure peak						Shattering of bubbles into localized "mists", seen in this and succeeding frames, persisting for 25-90 frames (2.5 msec - 9.0 msec); discrete bubbles no longer visible.

TABLE 2. Summary of Analysis of High Speed Cinematographic Records for EMI Test 18-4-85, for LGP 1845.

t (msec)	LIQUID PRESSURE (bar)	(kpsi)	(MPa)
0	1	0.015	0.1
0.1	200	2.94	20.3
0.2	545	8.01	55.2
0.3	967	14.21	97.7
0.4	1356	19.93	137.4
0.5	1600	23.52	162.1
0.6	1654	24.31	167.6

$$(dp/dt)_{max} = 61.0 \text{ kpsi/msec} = 420.5 \text{ MPa/msec}$$

$$(dp/dt)_{mean} = 15.7 \text{ kpsi/msec} = 108.2 \text{ MPa/msec}$$

TABLE 3. Tabulation of Pressure-Time Behavior for EMI Test 18-4-85, for LGP 1845.

LGP-1845

TEST NO.	INITIAL MEAN BUBBLE DIAMETER	INDIVIDUAL BUBBLE VOLUME	$(dp/dt)_{max}$		$(dp/dt)_{mean}$		PROPELLANT RESPONSE
	cm	cm^3	kpsi/msec	MPa/msec	kpsi/msec	MPa/msec	
EMI 18-4-85	$0.207 \leq D \leq 0.256$	$6.03 \times 10^{-3} \leq V \leq 1.07 \times 10^{-2}$	61.0	420.5	15.7	108.2	BENIGN
PCRL A13	$D \leq 0.0127$, distributed	$V \leq 1.07 \times 10^{-6}$	220.	1517.	32.0	220.6	BENIGN
PCRL A14	$D \leq 0.0127$, distributed	$V \leq 1.07 \times 10^{-6}$	220.	1517.	30.0	206.8	BENIGN
PCRL A20	$D \leq 0.0127$, distributed	$V \leq 1.07 \times 10^{-6}$	160.	1103.	43.	296.	EXPLOSION
PCRL A21	$D \leq 0.0127$, distributed	$V \leq 1.07 \times 10^{-6}$	110.	758.	45.	310.	BENIGN
PCRL A24	$D \leq 0.0127$, distributed	$V \leq 1.07 \times 10^{-6}$	87.	600.	39.	269.	EXPLOSION

TABLE 4. Summary of Comparative Analysis of Compression Ignition Tests for LGP 1845.

$(dp/dt)_{max}$ (est) $= 61.0$ kpsi/msec
$= 420.5$ MPa/msec

$(dp/dt)_{mean}$ (est) $= 15.7$ kpsi/msec
$= 108.2$ MPa/msec

Bubble No.	DIA (cm)	VOL (cm^3)	(V_o/V_b)	COMMENTS
t = 0				
1	0.0915	0.000401	1	Spherical, closely-packed bubbles
2	0.0976	0.000487	1	introduced in immediate vicinity
3	0.0793	0.000261	1	of bubble generator
4	0.0549	0.000087	1	
t = 0.0001	Field Pressure (est.) = 200 bar = 2.94 kpsi = 20.3 MPa			
1	0.0488	0.000061	6.574	Symmetric collapse; bubble no. 4
2	0.0732	0.000205	2.376	apparently merges with nearest
3	0.0305	0.000015	17.40	neighbors
4	--	--	--	
t = 0.0002	Field Pressure (est.) = 545 bar = 8.01 kpsi = 55.2 MPa			
1'	0.0366	0.000026		Bubbles no. 1 and 2 have merged
1''	0.0305	0.000015		and split into four smaller bubbles
1'''	0.0366	0.000026		
1''''	0.0366	0.000026		
3	0.0183	0.000003	29.0	
t = 0.0003	Field Pressure (est.) = 967 bar = 14.21 kpsi = 97.7 MPa			
				Bubble shattering; No measurable discrete bubbles; Collection of microbubbles in "mist-like" appearance persisting for 18 frames (1.8 msec)

TABLE 5. Summary of Analysis of High Speed Cinematographic Records for EMI Test 6-4-85, for NOS-365.

t (msec)	LIQUID PRESSURE (kpsi)	(MPa)
0	0.015	0.1
0.2	0.08	0.56
0.4	0.16	1.13
0.6	0.25	1.69
0.8	0.33	2.26
1.0	0.72	4.96
1.2	1.37	9.47
1.4	3.19	21.99
1.6	4.58	31.57
1.8	7.44	51.30

$$(dp/dt)_{max} \sim (dp/dt)_{mean} = 15.4 \text{ kpsi/msec}$$

$$= 106.1 \text{ MPa/msec}$$

TABLE 6. Tabulation of Pressure-Time Behavior for EMI Test 31-4-84, for NOS-365.

$(dp/dt)_{max}$ = 15.4 kpsi/msec
= 106.1 MPa/msec

$(dp/dt)_{mean}$ = 15.4 kpsi/msec
= 106.1 MPa/msec

Bubble No.	B H(cm)	A V(cm)	OBLATE SPHEROID VOL (cm^3)	(V_o/V_b)	PROLATE SPHEROID VOL (cm^3)	(V_o/V_b)	COMMENTS
t = 0							
1	0.1191	0.1191	0.000885	1	0.000885	1	Small bubbles located near center of field-of-view
2	0.1071	0.1071	0.000643	1	0.000643	1	
3	0.1191	0.1191	0.000885	1	0.000885	1	
4	0.1071	0.1131	0.000717	1	0.000679	1	
5	0.0714	0.0714	0.000191	1	0.000191	1	
6	0.0595	0.0595	0.000110	1	0.000110	1	
t = 0.0001 sec							
1	0.1191	0.1191	0.000885	1	0.000885	1	Collapse of individual bubbles; bubble boundary retains elliptical or spherical shape
2	0.0952	0.0952	0.000452	1.423	0.000452	1.423	
3	0.1191	0.1191	0.000885	1	0.000885	1	
4	0.1071	0.1131	0.000717	1	0.000679	1	
5	0.0714	0.0714	0.000191	1	0.000191	1	
6	0.0595	0.0595	0.000110	1	0.000110	1	
t = 0.0002 sec							
1	0.1071	0.1131	0.000717	1.234	0.000679	1.303	Collapse of individual bubbles; bubble boundary retains elliptical or spherical shape.
2	0.0952	0.0952	0.000452	1.423	0.000452	1.423	
3	0.1131	0.1071	0.000679	1.303	0.000717	1.234	
4	0.1021	0.1071	0.000608	1.179	0.000574	1.183	
5	0.0655	0.0655	0.000147	1.230	0.000147	1.230	
6	0.0595	0.0595	0.000110	1	0.000110	1	
t = 0.0003 sec							
1	0.0952	0.1102	0.000605	1.463	0.000523	1.692	Collapse of individual bubbles; bubble boundary retains elliptical or spherical shape.
2	0.0833	0.0893	0.000348	1.848	0.000324	1.985	
3	0.1012	0.1191	0.000752	1.177	0.000639	1.385	
4	0.0952	0.0952	0.000452	1.586	0.000452	1.502	
5	0.0595	0.0536	0.000090	2.122	0.000099	1.929	
6	0.0595	0.0536	0.000090	1.222	0.000099	1.111	
t = 0.0004 sec							
1	0.0893	0.0952	0.000424	2.087	0.000398	2.224	Collapse of individual bubbles; bubble boundary retains elliptical or spherical shape.
2	0.0714	0.0774	0.000224	2.871	0.000207	3.106	
3	0.0833	0.0833	0.000303	2.921	0.000303	2.921	
4	0.0833	0.0833	0.000303	2.366	0.000303	2.241	
5	0.0536	0.0476	0.000064	2.984	0.000072	2.653	
6	0.0476	0.0417	0.000043	2.558	0.000049	2.245	

TABLE 7. Summary of Analysis of High Speed Cinematographic Records for EMI Test 31-4-84, for NOS-365.

t = 0.0005 sec

Bubble No.	B H(cm)	A V(cm)	OBLATE SPHEROID VOL(cm^3)	(V_o/V_b)	PROLATE SPHEROID VOL(cm^3)	(V_o/V_b)	COMMENTS
1	0.0833	0.0833	0.000303	2.921	0.000303	2.921	Collapse of individual bubbles; bubble boundary retains elliptical or spherical shape.
2	0.0595	0.0833	0.000216	2.977	0.000154	4.175	
3	0.0833	0.0774	0.000261	3.391	0.000281	3.149	
4	0.0774	0.0774	0.000243	2.951	0.000243	2.794	
5	0.0476	0.0357	0.000032	5.969	0.000042	4.545	
6	0.0417	0.0357	0.000028	3.929	0.000033	3.333	

t = 0.0006 sec

Bubble No.	B H(cm)	A V(cm)	OBLATE SPHEROID VOL(cm^3)	(V_o/V_b)	PROLATE SPHEROID VOL(cm^3)	(V_o/V_b)	COMMENTS
1	0.0655	0.0833	0.000238	3.718	0.000187	4.733	Collapse of individual bubbles; bubble boundary retains elliptical or spherical shape.
2	0.0536	0.0536	0.000081	7.938	0.000081	7.938	
3	0.0774	0.0655	0.000174	5.086	0.000205	4.317	
4	0.0655	0.0655	0.000147	4.878	0.000147	4.619	
5	0.0357	0.0357	0.000024	7.958	0.000024	7.958	
6	0.0357	0.0298	0.000017	6.471	0.000020	5.500	

t = 0.0007 sec

Bubble No.	B H(cm)	A V(cm)	OBLATE SPHEROID VOL(cm^3)	(V_o/V_b)	PROLATE SPHEROID VOL(cm^3)	(V_o/V_b)	COMMENTS
1	0.0476	0.0655	0.000107	8.271	0.000078	11.346	Collapse of individual bubbles; bubble boundary retains elliptical or spherical shape.
2	0.0476	0.0536	0.000072	8.931	0.000064	10.047	
3	0.0714	0.0595	0.000132	6.705	0.000159	5.566	
4	0.0536	0.0476	0.000064	11.203	0.000072	9.431	
5	0.0298	0.0298	0.000014	13.643	0.000014	13.643	
6	0.0357	0.0298	0.000017	6.471	0.000020	5.500	

t = 0.0008 sec

Bubble No.	B H(cm)	A V(cm)	OBLATE SPHEROID VOL(cm^3)	(V_o/V_b)	PROLATE SPHEROID VOL(cm^3)	(V_o/V_b)	COMMENTS
1	0.0476	0.0595	0.000088	10.057	0.000071	12.465	Collapse of individual bubbles; bubble boundary retains elliptical or spherical shape
2	0.0476	0.0476	0.000056	11.482	0.000056	11.482	
3	0.0595	0.0536	0.000090	9.833	0.000099	8.939	
4	0.0417	0.0357	0.000028	25.607	0.000033	20.576	
5	0.0238	0.0238	0.000007	27.286	0.000007	27.286	
6	0.0298	0.0238	0.000009	12.222	0.000011	10.000	

t = 0.0009 sec

Bubble No.	B H(cm)	A V(cm)	OBLATE SPHEROID VOL(cm^3)	(V_o/V_b)	PROLATE SPHEROID VOL(cm^3)	(V_o/V_b)	COMMENTS
1	0.0357	0.0476	0.000042	21.071	0.000032	27.656	Continual collapse of bubbles; persists for 31 frames (3.1 msec).
2	0.0357	0.0357	0.000024	26.792	0.000024	26.792	
3	0.0476	0.0417	0.000043	20.581	0.000049	18.061	
4	0.0357	0.0357	0.000024	29.875	0.000024	28.292	
5	0.0238	0.0238	0.000007	27.286	0.000007	27.286	
6	0.0298	0.0238	0.000009	12.222	0.000011	10.000	

TABLE 7. (Cont'd.)

NOS-365

TEST NO.	INITIAL MEAN BUBBLE DIAMETER	INDIVIDUAL BUBBLE VOLUME	$(dp/dt)_{max}$		$(dp/dt)_{mean}$		PROPELLANT RESPONSE
	cm	cm^3	kpsi/msec	MPa/msec	kpsi/msec	MPa/msec	
EMI 6-4-85	$0.0549 \leq D \leq 0.0915$	$8.70 \times 10^{-5} \leq V \leq 4.87 \times 10^{-4}$	61.0	420.5	15.7	108.2	BENIGN
EMI 31-4-84	$0.0595 \leq D \leq 0.1191$	$1.10 \times 10^{-4} \leq V \leq 8.85 \times 10^{-4}$	15.4	106.1	15.4	106.1	BENIGN
PCRL LP06	$D \leq 0.0025$, distributed	$V \leq 8.18 \times 10^{-6}$	$200.^{est}$	$1500.^{est}$	$30.^{est}$	$200.^{est}$	BENIGN
PCRL LP07	$D \leq 0.0025$, distributed	$V \leq 8.18 \times 10^{-6}$	$200.^{est}$	$1500.^{est}$	$30.^{est}$	$200.^{est}$	BENIGN
PCRL LP15	$D \leq 0.0025$, distributed	$V \leq 8.18 \times 10^{-6}$	$120.^{est}$	$800.^{est}$	$40.^{est}$	$300.^{est}$	EXPLOSION
PCRL LP16	$D \leq 0.0025$, distributed	$V \leq 8.18 \times 10^{-6}$	$120.^{est}$	$800.^{est}$	$40.^{est}$	$300.^{est}$	BENIGN
PCRL LP17	$D \leq 0.0025$, distributed	$V \leq 8.18 \times 10^{-6}$	$120.^{est}$	$800.^{est}$	$40.^{est}$	$300.^{est}$	EXPLOSION
PCRL LP18	$D \leq 0.0025$, distributed	$V \leq 8.18 \times 10^{-6}$	$120.^{est}$	$800.^{est}$	$40.^{est}$	$300.^{est}$	EXPLOSION

TABLE 8. Summary of Comparative Analysis of Compression Ignition Tests for NOS-365.

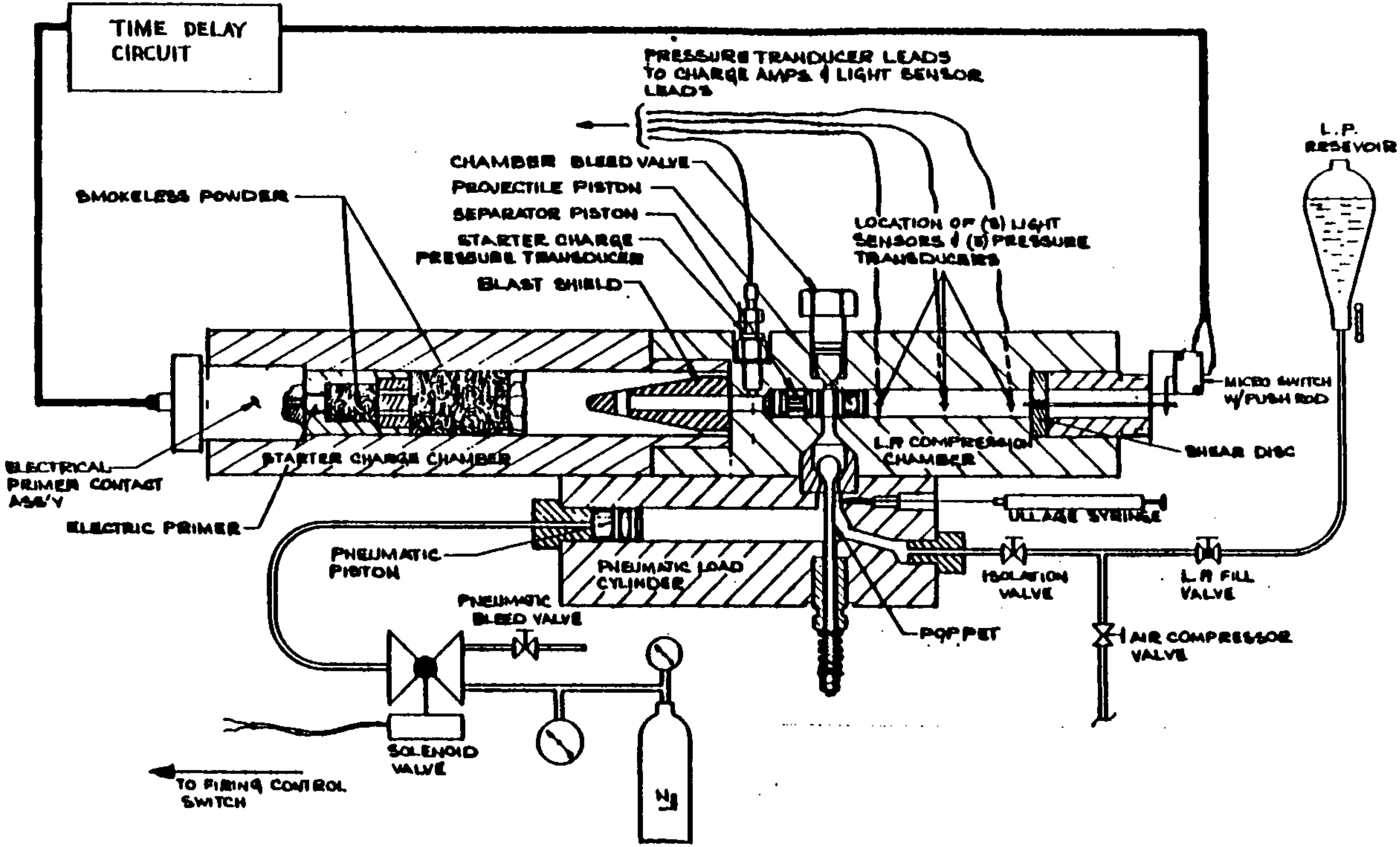

FIGURE 1. Schematic Drawing of PCRL Compression Ignition Sensitivity Test Fixture.

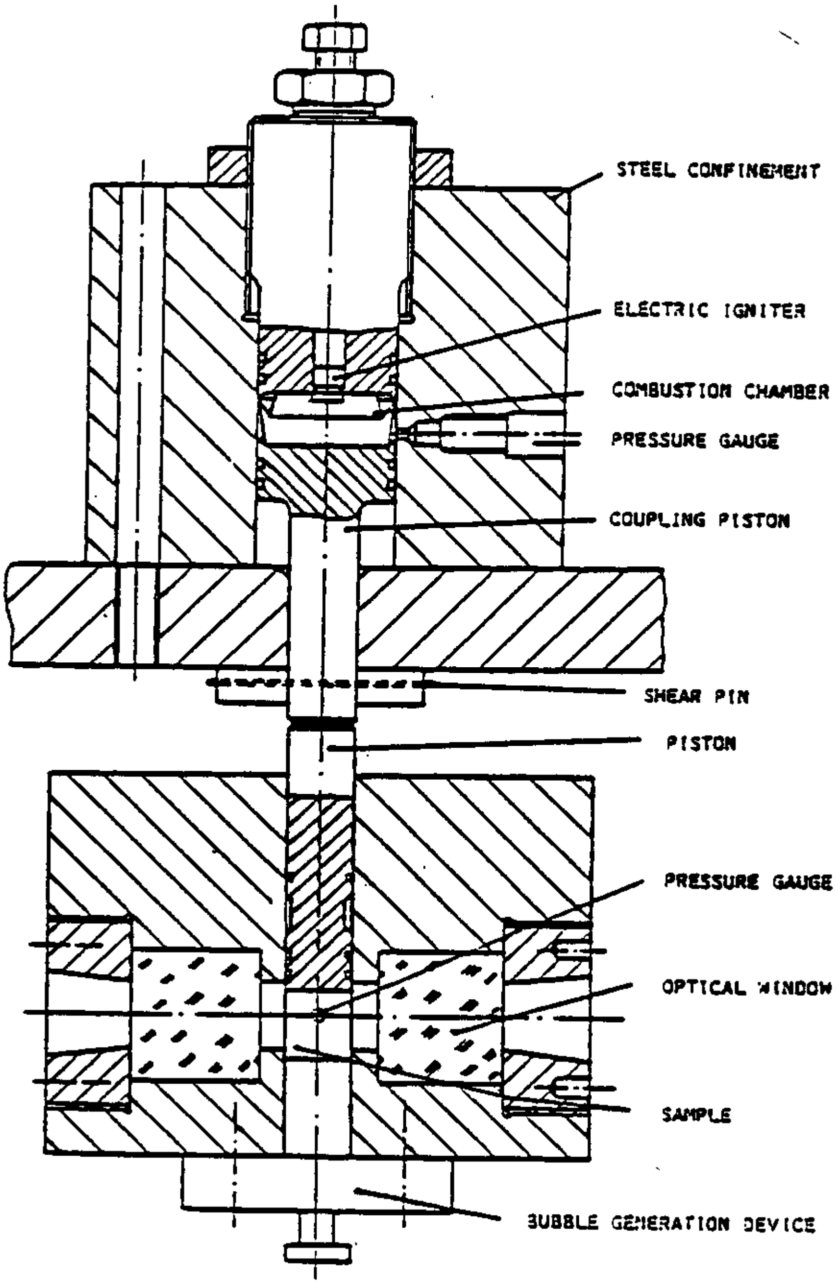

FIGURE 2. Schematic Drawing of EMI-AFB Compression Test Fixture.

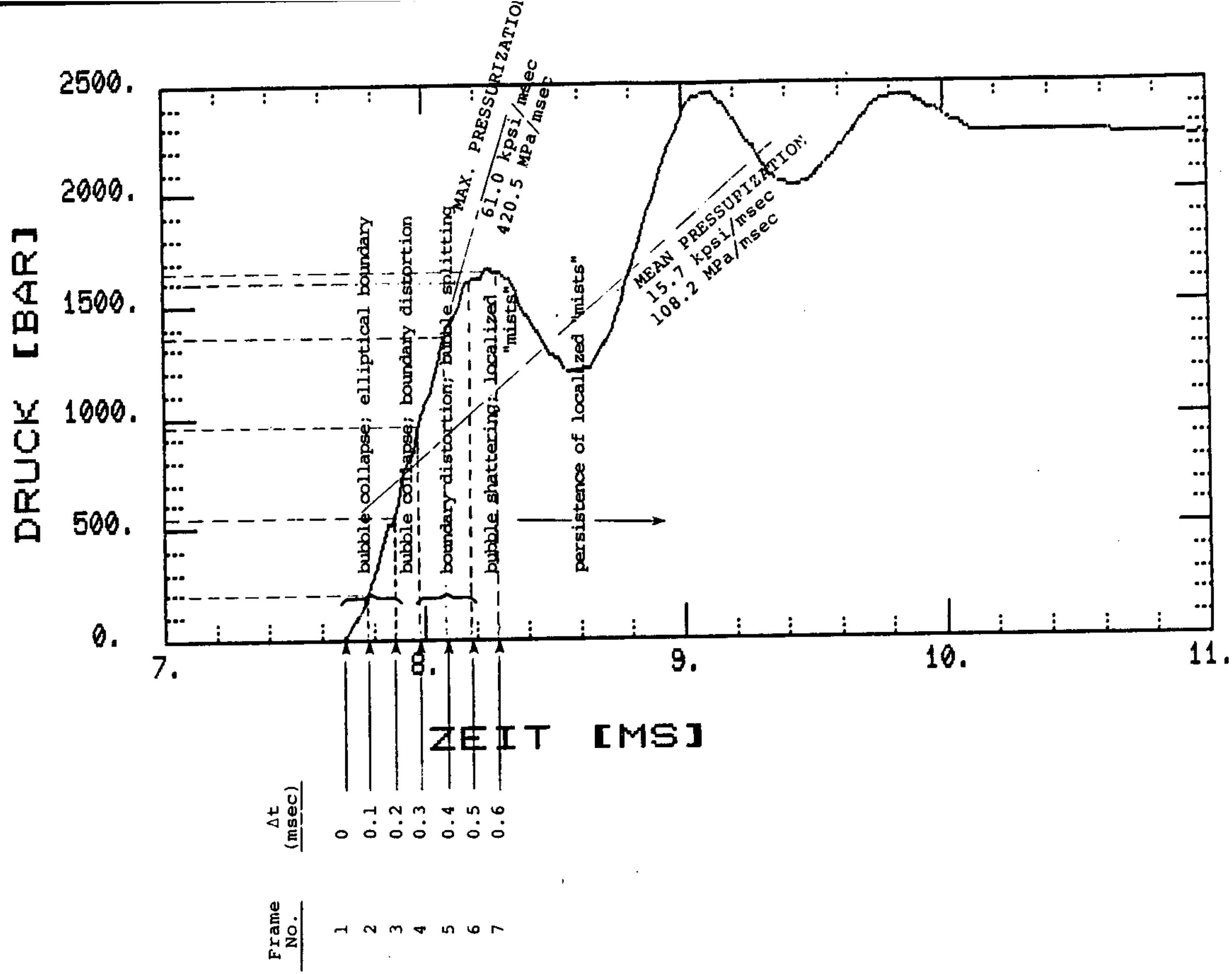

FIGURE 3. Expanded Plot of Pressure-Time Behavior in EMI Test 18-4-85, for LGP 1845.

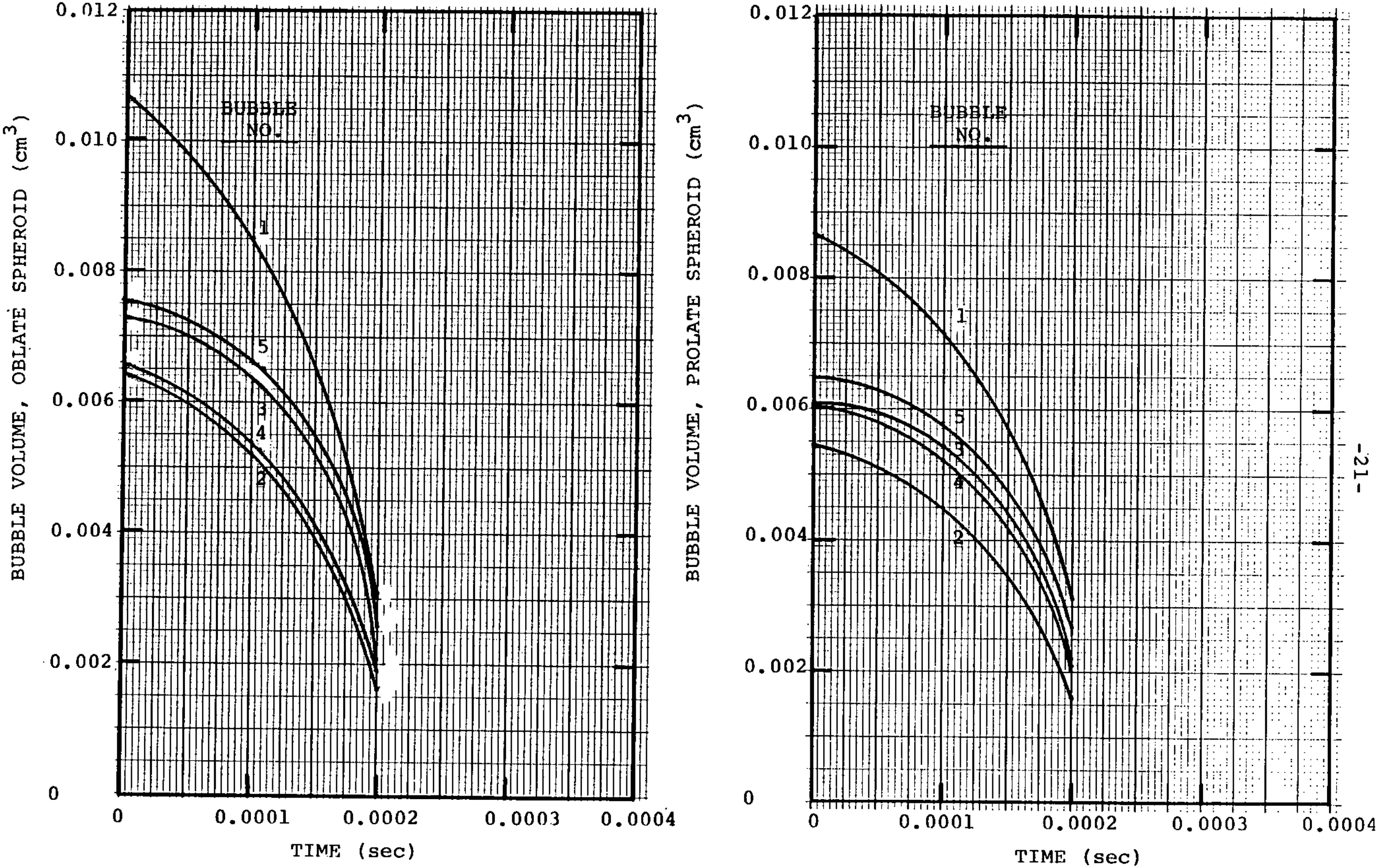

FIGURE 4. Volumetric Compression of the Individual Bubbles in EMI Test 18-4-85. for LPG-1845. No Measurements Were Made for t>0.0002 sec Due to Boundary Distortion.

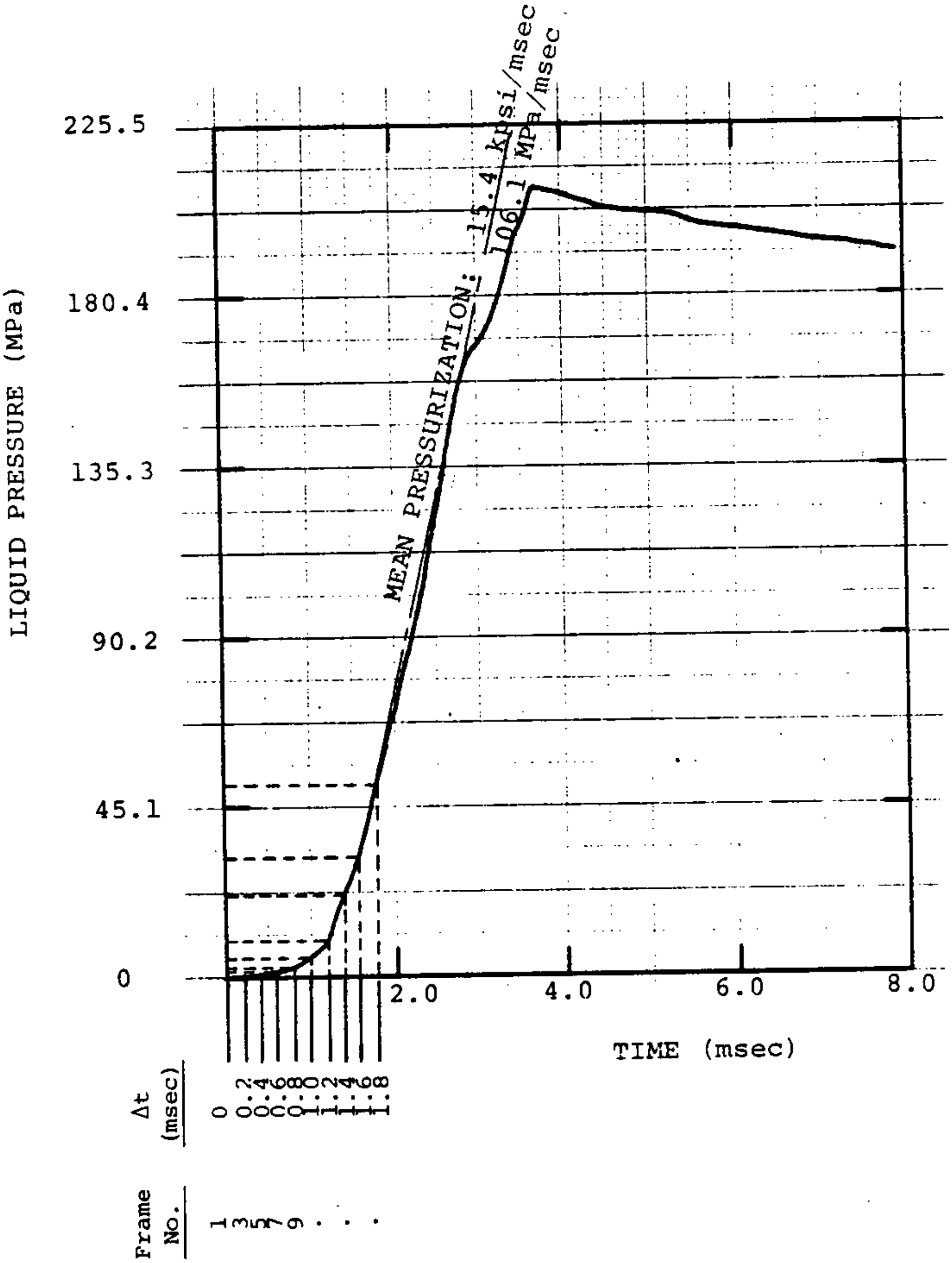

FIGURE 5. Plot of Pressure-Time Behavior in EMI Test 31-4-84, for NOS-365.

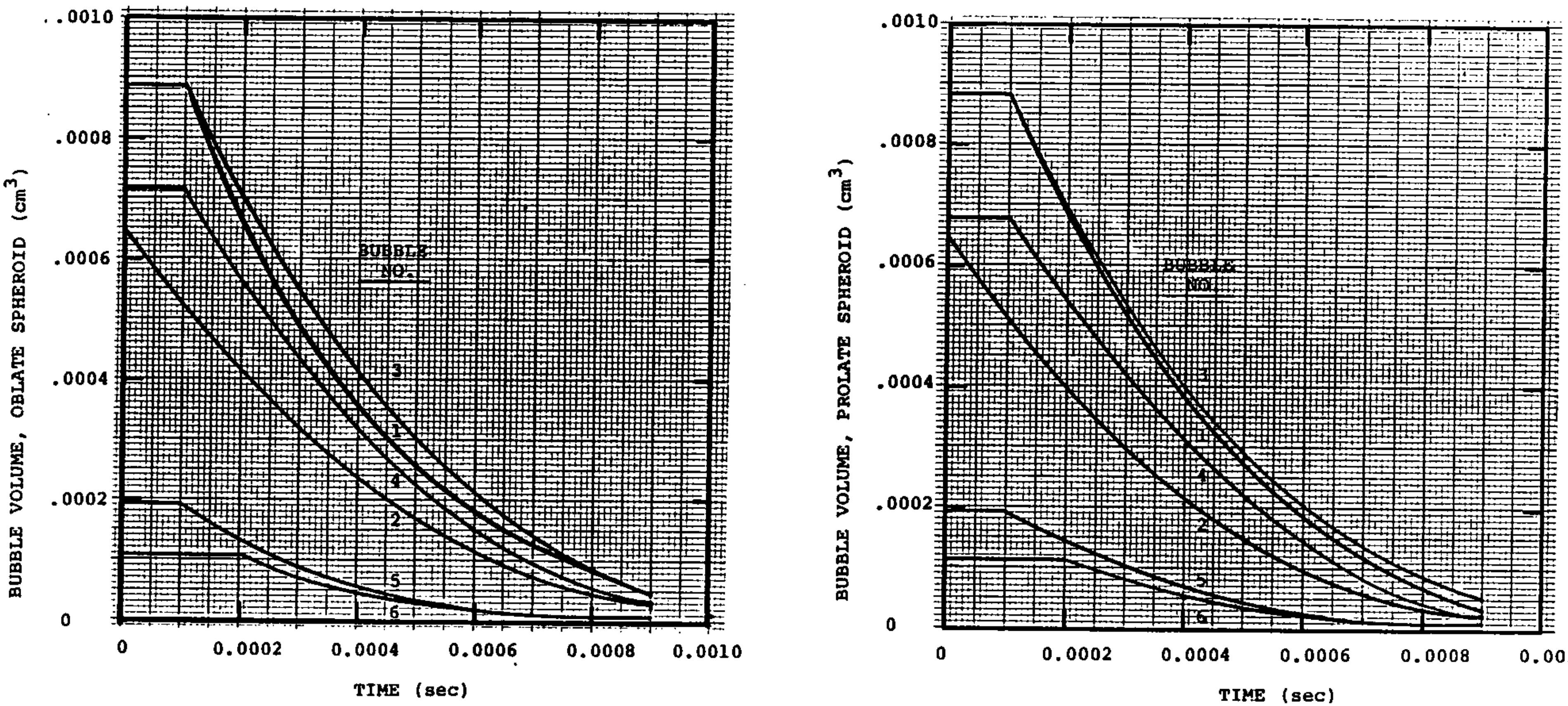

FIGURE 6. Volumetric Compression of the Individual Bubbles in EMI Test 31-4-84, for NOS-365. No Measurements Were Made for t>0.0009 sec.

DISTRIBUTION LIST

No. of Copies	Organization
12	Commander Defense Technical Info Center ATTN: DTIC-DDA Cameron Station Alexandria, VA 22304-6145
1	Director Defense Advanced Research Projects Agency ATTN: H. Fair 1400 Wilson Boulevard Arlington, VA 22209
1	HQDA DAMA-ART-M Washington, DC 20310
1	Commander US Army Materiel Command ATTN: AMCDRA-ST 5001 Eisenhower Avenue Alexandria, VA 22333-0001
13	Commander Armament R&D Center US Army AMCCOM ATTN: SMCAR-TSS SMCAR-TDC SMCAR-SCA, B. Brodman R. Yalamanchili SMCAR-AEE-B, D. Downs A. Beardell SMCAR-LCE, N. Slagg SMCAR-AEE-B, W. Quine A. Bracuti J. Lannon SMCAR-CCH, R. Price SMCAR-FSS-A, L. Frauen SMCAR-FSA-S, H. Liberman Picatinny Arsenal, NJ 07806-5000
3	Director Benet Weapons Laboratory Armament R&D Center US Army AMCCOM ATTN: SMCAR-LCB-TL E. Conroy A. Graham Watervliet, NY 12189
1	Commander US Army Armament, Munitions and Chemical Command ATTN: SMCAR-ESP-L Rock Island, IL 61299-7300
1	Commander US Army Aviation Research and Development Command ATTN: AMSAV-E 4300 Goodfellow Blvd St. Louis, MO 63120
1	Commander Materials Technology Lab US Army Laboratory Cmd ATTN: SLCMT-MCM-SB M. Levy Watertown, MA 02172-0001
1	Director US Army Air Mobility Rsch and Development Lab Ames Research Center Moffett Field, CA 94035
1	Commander US Army Communications Electronics Command ATTN: AMSEL-ED Fort Monmouth, NJ 07703

DISTRIBUTION LIST

No. of Copies	Organization
1	Commander ERADCOM Technical Library ATTN: STET-L Ft. Monmouth, NJ 07703-5301
1	Commander US Army Harry Diamond Labs ATTN: SLCHD-TA-L 2800 Powder Mill Rd Adelphi, MD 20783
1	Commander US Army Missile Command Rsch, Dev, & Engr Ctr ATTN: AMSMI-RD Redstone Arsenal, AL 35898
1	Commander US Army Missile & Space Intelligence Center ATTN: AIAMS-YDL Redstone Arsenal, AL 35898-5500
1	Commander US Army Belvoir R&D Ctr ATTN: STRBE-WC Tech Library (Vault) B-315 Fort Belvoir, VA 22060-5606
1	Commander US Army Tank Automotive Cmd ATTN: AMSTA-TSL Warren, MI 48397-5000
1	Commander US Army Research Office ATTN: Tech Library PO Box 12211 Research Triangle Park, NC 27709-2211

No. of Copies	Organization
1	Director US Army TRADOC Systems Analysis Activity ATTN: ATAA-SL White Sands Missile Range NM 88002
1	Commandant US Army Infantry School ATTN: ATSH-CD-CSO-OR Fort Benning, GA 31905
1	Commander Armament Rsch & Dev Ctr US Army Armament, Munitions and Chemical Command ATTN: SMCAR-CCS-C, T Hung Picatinny Arsenal, NJ 07806-5000
1	Commandant US Army Field Artillery School ATTN: ATSF-CMW Ft Sill, OK 73503
1	Commandant US Army Armor Center ATTN: ATSB-CD-MLD Ft Knox, KY 40121
1	Commander US Army Development and Employment Agency ATTN: MODE-TED-SAB Fort Lewis, WA 98433
1	Commander Naval Surface Weapons Center ATTN: D.A. Wilson, Code G31 Dahlgren, VA 22448-5000
1	Commander Naval Surface Weapons Center ATTN: Code G33, J. East Dahlgren, VA 22448-5000

DISTRIBUTION LIST

No. of Copies	Organization
2	Commander US Naval Surface Weapons Ctr ATTN: O. Dengel K. Thorsted Silver Spring, MD 20902-5000
1	Commander Naval Weapons Center China Lake, CA 93555-6001
1	Commander Naval Ordnance Station ATTN: C. Dale Code 5251 Indian Head, MD 20640
1	Superintendent Naval Postgraduate School Dept of Mechanical Engr ATTN: Code 1424, Library Monterey, CA 93943
1	AFWL/SUL Kirtland AFB, NM 87117
1	Air Force Armament Lab ATTN: AFATL/DLODL Eglin AFB, FL 32542-5000
1	AFOSR/NA (L. Caveny) Bldg 410 Bolling AFB, DC 20332
1	Commandant USAFAS ATTN: ATSF-TSM-CN Ft Sill, OK 73503-5600
1	US Bureau of Mines ATTN: R.A. Watson 4800 Forbes Street Pittsburgh, PA 15213

No. of Copies	Organization
1	Director Jet Propulsion Lab ATTN: Tech Library 4800 Oak Grove Drive Pasadena, CA 91109
2	Director National Aeronautics and Space Administration ATTN: MS-603, Tech Lib MS-86, Dr. Povinelli 21000 Brookpark Road Lewis Research Center Cleveland, OH 44135
1	Director National Aeronautics and Space Administration Manned Spacecraft Center Houston, TX 77058
10	Central Intelligence Agency Office of Central Reference Dissemination Branch Room GE-47 HQS Washington, DC 20502
1	Central Intelligence Agency ATTN: Joseph E. Backofen HQ Room 5F22 Washington, DC 20505
3	Bell Aerospace Textron ATTN: F. Boorady F. Picirillo A.J. Friona PO Box One Buffalo, NY 14240
1	Calspan Corporation ATTN: Tech Library PO Box 400 Buffalo, NY 14225

DISTRIBUTION LIST

No. of Copies	Organization
7	General Electric Ord Sys Div ATTN: J. Mandzy, OP43-220 R.E. Mayer H. West M. Bulman R. Pate I. Magoon J. Scudiere 100 Plastics Avenue Pittsfield, MA 01201-3698
1	General Electric Company Armament Systems Department ATTN: D. Maher Burlington, VT 05401
1	IITRI ATTN: Library 10 W. 35th St Chicago, IL 60616
1	Olin Chemicals Research ATTN: David Gavin PO Box 586 Chesire, CT 06410-0586
2	Olin Corporation ATTN: Victor A. Corso Dr. Ronald L. Dotson PO Box 30-9644 New Haven, CT 06536
1	Paul Gough Associates ATTN: Paul Gough PO Box 1614 Portsmouth, NH 03801
1	Safety Consulting Engr ATTN: Mr. C. James Dahn 5240 Pearl St Rosemont, IL 60018

No. of Copies	Organization
1	Science Applications, Inc. ATTN: R. Edelman 23146 Cumorah Crest Woodland Hills, CA 91364
1	Sundstrand Aviation Operations ATTN: Mr. Owen Briles PO Box 7202 Rockford, IL 61125
1	Veritay Technology, Inc. ATTN: E.B. Fisher 4845 Millersport Highway PO Box 305 East Amherst, NY 14051-0305
1	Director Applied Physics Laboratory The Johns Hopkins Univ. Johns Hopkins Road Laurel, MD 20707
2	Director CPIA The Johns Hopkins Univ. ATTN: T. Christian Tech Library Johns Hopkins Road Laurel, MD 20707
1	U. of Illinois at Chicago ATTN: Professor Sohail Murad Dept of Chemical Engr Box 4348 Chicago, IL 60680
1	U. of MD at College Park ATTN: Professor Franz Kasler Department of Chemistry College Park, MD 20742

DISTRIBUTION LIST

No. of Copies	Organization
1	U. of Missouri at Columbia ATTN: Professor R. Thompson Department of Chemistry Columbia, MO 65211
1	U. of Michigan ATTN: Prof. Gerard M. Faeth Dept of Aerospace Engr Ann Arbor, MI 48109-3796
1	U. of Missouri at Columbia ATTN: Professor F.K. Ross Research Reactor Columbia, MO 65211
1	U. of Missouri at Kansas City Department of Physics ATTN: Prof. R.D. Murphy 1110 East 48th Street Kansas City, MO 64110-2499
1	Pennsylvania State University Dept of Mechanical Engr ATTN: Prof. K. Kuo University Park, PA 16802
2	Princeton Combustion Rsch Laboratories, Inc. ATTN: N.A. Messina M. Summerfield 475 US Highway One North Monmouth Junction, NJ 08852
1	University of Arkansas Dept of Chemical Engr ATTN: J. Havens 227 Engineering Building Fayetteville, AR 72701

No. of Copies	Organization
3	University of Delaware Department of Chemistry ATTN: Mr. James Cronin Professor Thomas Brill Mr. Peter Spohn Newark, DE 19711

Aberdeen Proving Ground

	Dir, USAMSAA ATTN: AMXSY-D AMXSY-MP, H. Cohen
	Cdr, USATECOM ATTN: AMSTE-TO-F
	Cdr, CRDEC, AMCCOM ATTN: SMCCR-RSP-A SMCCR-MU SMCCR-SPS-IL

USER EVALUATION SHEET/CHANGE OF ADDRESS

This Laboratory undertakes a continuing effort to improve the quality of the reports it publishes. Your comments/answers to the items/questions below will aid us in our efforts.

1. BRL Report Number ______________________ Date of Report ______________

2. Date Report Received ____

3. Does this report satisfy a need? (Comment on purpose, related project, or other area of interest for which the report will be used.) ______________

4. How specifically, is the report being used? (Information source, design data, procedure, source of ideas, etc.) ______________

5. Has the information in this report led to any quantitative savings as far as man-hours or dollars saved, operating costs avoided or efficiencies achieved, etc? If so, please elaborate. ______________

6. General Comments. What do you think should be changed to improve future reports? (Indicate changes to organization, technical content, format, etc.)

CURRENT ADDRESS

Name

Organization

Address

City, State, Zip

7. If indicating a Change of Address or Address Correction, please provide the New or Correct Address in Block 6 above and the Old or Incorrect address below.

OLD ADDRESS

Name

Organization

Address

City, State, Zip

(Remove this sheet, fold as indicated, staple or tape closed, and mail.)

— — — — — — — — — — FOLD HERE — — — — — — — — — —

Director
U.S. Army Ballistic Research Laboratory
ATTN: SLCBR-DD-T
Aberdeen Proving Ground, MD 21005-5066

NO POSTAGE
NECESSARY
IF MAILED
IN THE
UNITED STATES

OFFICIAL BUSINESS
PENALTY FOR PRIVATE USE, $300

BUSINESS REPLY MAIL
FIRST CLASS PERMIT NO 12062 WASHINGTON, DC

POSTAGE WILL BE PAID BY DEPARTMENT OF THE ARMY

Director
U.S. Army Ballistic Research Laboratory
ATTN: SLCBR-DD-T
Aberdeen Proving Ground, MD 21005-9989

— — — — — — — — — — FOLD HERE — — — — — — — — — —